Development of a Compact Hard X-Ray Camera on the TST-2 Spherical Tokamak

Akira EJIRI, Yuki AOI, Hibiki YAMAZAKI, Naoto TSUJII, Yuichi TAKASE, Osamu WATANABE, Yongtae KO, James H.P. RICE, Yi PENG, Kotaro IWASAKI, Kyohei MATSUZAKI, Yuki OSAWA and Yasuo YOSHIMURA[1)]

The University of Tokyo, Kashiwa 277-8561, Japan
[1)]*National Institute for Fusion Science, Toki 509-5292, Japan*

(Received 26 February 2020 / Accepted 15 March 2020)

A compact hard X-ray camera has been developed to study the behavior of fast electrons accelerated by lower hybrid waves in the TST-2 spherical tokamak. The camera consists of a pinhole made of tungsten alloy, a thin resin window, a thin LYSO scintillator disk, 5 fiber optic light guides and 5 photomultiplier tubes and shields. The camera is installed on a tangential port, and two-dimensional images are obtained by rotating the system around the axis of the port on a shot by shot basis. The typical energy range is 10 - 250 keV, and the energy resolution is about 100% (FWHM) at 100 keV. The measured images of a lower hybrid wave driven plasma show bright region at the inboard side (i.e., high field side).

Keywords: hard X-ray measurement, pinhole camera, LYSO scintillator, spherical tokamak, lower hybrid wave

DOI: 10.1585/pfr.15.1202023

Plasma current start-up and sustainment by lower hybrid waves (LHWs) with a frequency of 200 MHz have been studied in the TST-2 spherical tokamak device [1, 2]. Hard X-ray emission contains information on the fast electrons, and space, time and energy resolved measurements would be a powerful tool to study the wave physics, including current drive mechanisms. In this paper, we report the development of a compact tangential hard X-ray camera with a moderate space, time and energy resolutions.

Since the maximum observed energy is a few hundred of keV [3] and semiconductor detector signals are often contaminated by RF noise, we chose the combination of a scintillator and photomultiplier tubes (PMTs). In order to realize a two-dimensional measurement on a tangential view, we adopt a pinhole camera configuration with a thin LYSO scintillator disk (Fig. 1). A pinhole (ϕ2) made of tungsten alloy is placed inside the tangential port. The X-rays pass through the pinhole and a thick (t3) poly ether ether ketone (PEEK) vacuum window, and they hit a thin LYSO scintillator disk (ϕ60, t1) generating scintillation light. Five light guides (ϕ6.3 × 1.8 m) are attached on the back side of the disk and the scintillation light is transferred to a PMT located far from the device to avoid the sensitivity deterioration by the magnetic fields.

The energy range depends on the PEEK window and the LYSO thicknesses, and it becomes about 10 - 250 keV, if we impose a scintillator absorption efficiency higher than 20%. A radio isotope element ^{176}Lu is contained in the LYSO scintillator, but the count rate due to the element is negligible compared with those by plasma.

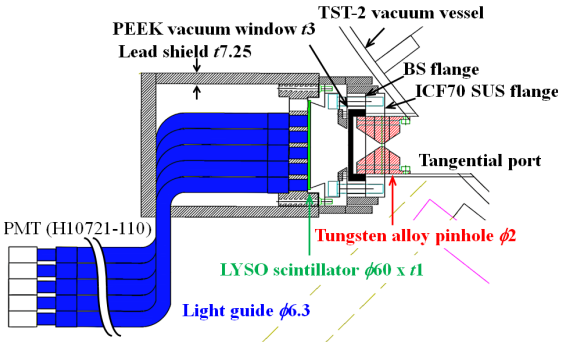

Fig. 1 Cross section of the compact hard X-ray pinhole camera installed at a tangential port of the TST-2 device.

A thicker scintillator is preferable for higher efficiency at high energies, but a thick scintillator induces a wider spread of scintillation light. The spread was measured by a combination of a fixed radio isotope source (ϕ1) and a detector (ϕ1) moving on the scintillator surface. The FWHMs of count rate profile are 1.4 and 2.8 mm for the scintillator thicknesses of 1 and 3 mm, respectively and we chose the former. In the present configuration, the spatial resolution is determined mainly by the diameter (ϕ6.3) of a light guide, and the radial spread of each viewing sight in the plasma is about 0.06 m. The 5 viewing sights cover the radial regions of about 0.185 - 0.646 m, while the inboard and outboard limiters are located at R = 0.13 m and 0.585 m, respectively. The light guides are fixed by a lead

author's e-mail: ejiri@k.u-tokyo.ac.jp

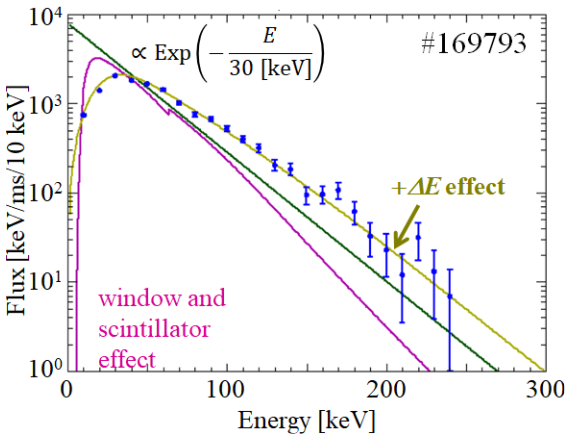

Fig. 2 A typical measured energy spectrum (symbols) and the obtained original spectrum (green), the spectrum with window and scintillator effect (magenta) and a spectrum with all effects (olive).

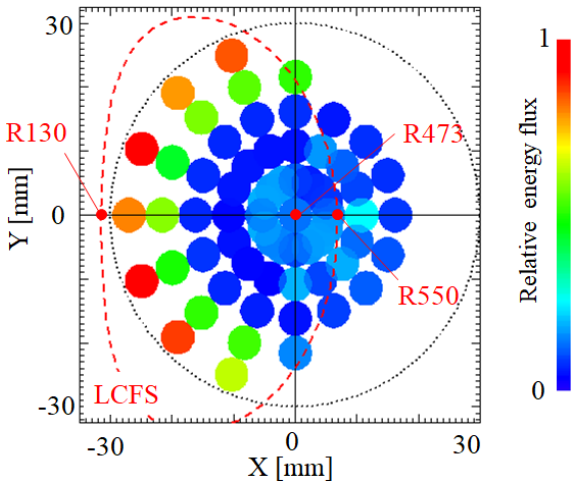

Fig. 3 Color map of the hard X-ray energy flux on the scintillation disk (dotted circle) obtained from 16 reproducible discharges. X and Y show the horizontal and vertical coordinates on the scintillator disk. The plotted circle diameter (ϕ5.4) is smaller than the actual light guide core diameter (ϕ6.3) for better visibility. The dashed curve shows the projection of LCFS on a poloidal plane, where R473 represents the tangent point of the central line of sight with tangent radius of R = 473 mm. R130 and R550 represent the major radii on the poloidal plane.

holder. By using another holder, we can make additional 4 viewing sights, and 9 viewing sights in total are available. The system can be rotated around the axis of the camera on a shot by shot base.

The scintillator is surrounded by shield components made of lead, brass, stainless steel or tungsten alloy to reduce the stray X-rays, which do not pass through the pinhole. Note that there is a significant X-ray flux from the backside of the system, and such flux is significantly reduced by lead components on the backside. The effect of such stray X-rays is estimated by the comparison of a normal measurement and a measurement with a lead blocking plate in front of the scintillator. Typical stray X-ray ratio is about 1/5 at ~ 10 keV and 1/200 at 100 keV. The higher stray X-ray ratio for lower energy probably reflects the low energy stray X-rays generated through multiple reflection or scattering of higher energy X-rays. There is a pass for X-ray to hit the scintillator through stainless steel components and we often add a thin lead sheet to reduce the stray light through the component.

A preamplifier (active I-V convertor) is used for each PMT, and the FWHM of the output pulse is 1.2 µs. The sensitivity (energy/pulse height) and the energy resolution is measured by using radio isotopes: ^{57}Co (122 keV) and ^{133}Ba (356 keV). The energy resolution shows a $E^{1/2}$ dependence, where E is the X-ray energy, and the FWHM resolution is about 100% at 100 keV.

Figure 2 shows a typical energy spectrum of the detected X-rays from an LHW sustained plasma with a plasma current of 18 kA, an LHW injection power of 55 kW and a line average electron density of about 4×10^{17} m^{-3}. The accumulation time for this spectrum is 10 ms. The detection efficiency is affected by window transmission and scintillator absorption, and the detected energy is affected by finite energy resolution. We consider these effects assuming an Maxwellian shape for the original energy spectrum. The effect of the energy resolution is taken into account by convolving the resolution. In practice, we fit the measured spectrum with a calculated one, and obtain the effective temperature of the Maxwellian distribution.

Two dimensional hard X-ray images of the tangential view are obtained from 16 (= 2 × 8 angles) reproducible discharges sustained by LHW. Figure 3 shows the color map (i.e., intensity map) of the detected hard X-ray energy flux on the scintillator. The accumulation (i.e., analysis) time is 1.2 ms for this case. The projection of the last closed flux surface (LCFS) obtained from an equilibrium reconstruction for one of those discharges is also plotted. The left intense region corresponds to the inboard midplane region. One of the possible reasons for the higher intensity for the inboard side is that fast electrons spend longer time at the inboard side due to the low aspect ratio magnetic configuration.

In summary, we have developed a compact hard X-ray pinhole camera and installed on a tangential port of the TST-2 spherical tokamak device. LHW sustained plasmas are measured. Two-dimensional image of a tangential view is obtained, showing intense emission at the inboard side.

This work is partly supported by National Institute for Fusion Science Collaboration Research Program NIFS18KOAR022 and NIFS12KUTR078.

[1] Y. Takase *et al.*, Nucl. Fusion **41**, 1543 (2001).
[2] S. Yajima *et al.*, Plasma Fusion Res. **13**, 3402114 (2018).
[3] H. Togashi *et al.*, Plasma Fusion Res. **12**, 1402030 (2017).